Eur Biophys J (2005) 34: 28–41
DOI 10.1007/s00249-004-0422-3

ARTICLE

**Klaus Brandenburg · Patrick Garidel
Andra B. Schromm · Jörg Andrä · Arjen Kramer
Maarten Egmond · Andre Wiese**

Investigation into the interaction of the bacterial protease OmpT with outer membrane lipids and biological activity of OmpT:lipopolysaccharide complexes

Received: 19 February 2004 / Revised: 4 May 2004 / Accepted: 17 May 2004 / Published online: 6 July 2004

Abstract Outer-membrane proteases T (OmpT) are important defence molecules of Gram-negative bacteria such as *Escherichia coli* found in particular in clinical isolates. We studied the interaction of OmpT with the membrane-forming lipids phosphatidylethanolamine (PE) and phosphatidylglycerol (PG) from the inner leaflet and lipopolysaccharide (LPS) from the outer leaflet of the outer membrane. These investigations comprise functional aspects of the protein–lipid interaction mimicking the outer-membrane system as well as the bioactivity of LPS:OmpT complexes in the infected host after release from the bacterial surface. The molecular interaction of the lipids PE, PG, and LPS with OmpT was investigated by analysing molecular groups in the lipids originating from the apolar region (methylene groups), the interface region (ester), and the polar region (phosphates), and by analysing the acyl-chain melting-phase behaviour of the lipids. The activity of OmpT and LPS:OmpT complexes was investigated in biological test systems (human mononuclear cells and *Limulus* amoebocyte lysate assay) and with phospholipid model membranes. The results show a strong influence of OmpT on the mobility of the lipids leading to a considerable fluidization of the acyl chains of the phospholipids as well as LPS, and a rigidification of the phospholipid, but not LPS head groups. From this, a dominant role of the protein on the function of the outer membrane can be deduced. OmpT released from the outer membrane still contains slight contaminations of LPS, but its strong cytokine-inducing ability in mononuclear cells, which does not depend on the Toll-like receptors 2 and 4, indicates an LPS-independent mechanism of cell activation. This might be of general importance for infections induced by Gram-negative bacteria.

Keywords OmpT · LPS · Cytokine induction · Membrane fluidity · Outer membrane

K. Brandenburg (✉) · A. B. Schromm · J. Andrä · A. Wiese
Forschungszentrum Borstel, Div. of Biophysics,
Leibniz-Institut für Medizin und Biowissenschaften,
Parkallee 10, 23845 Borstel, Germany
E-mail: Kbranden@fz-borstel.de
Tel.: +49-4537-188235
Fax: +49-4537-188632

P. Garidel
Institut für Physikalische Chemie,
Martin-Luther Universität Halle-Wittenberg,
06108 Halle, Germany

A. Kramer · M. Egmond
Centre for Biomembranes and Lipid Enzymology,
Universiteit Utrecht, Utrecht, The Netherlands

Introduction

The outer-membrane protease OmpT, a 33.3-kDa serine protease of 297 amino acid residues, belongs to the family of the omptins including the proteases PgtE from *Salmonella thyphimurium* (mature protein has 49% identity with OmpT), Pla from *Yersinia pestis* (50% identity) and OmpP from *Escherichia coli* (72% identity). The OmpT proteases, which cleave peptides and proteins preferentially between two consecutive basic amino acid residues (Sugimura and Nishihara 1988; Kramer et al. 2000, 2001; Dekker et al. 2001), have been suggested to be involved, for example, in urinary tract disease (Webb and Lundrigan 1996), since *ompT* genes were found in clinical isolates of *E.coli*. Also, it has been proposed that OmpT participates in the degradation of antimicrobial peptides secreted by epithelial cells from the urinary tract (Stumpe et al. 1998), which is supported by the observation that the antimicrobial peptide protamine could be degraded by OmpT (Stumpe et al. 1998). However, the general biological function of OmpT still remains to be elucidated.

For the proper function of outer-membrane proteins (Omp), the properties of the matrix lipids embedding the latter are of importance as has been shown for porins (Wiese et al. 1994). A mixture of phosphatidylethanol-

amine (PE), phosphatidylglycerol (PG), and cardiolipin in a molar ratio of 87:12:1 forms the inner leaflet of the outer membrane, whereas lipopolysaccharide (LPS) is the exclusive lipid of the outer leaflet, i.e. the outer membrane is strongly asymmetric (Nikaido and Vaara 1985). It was found that the intercalation of the porins OmpC and OmpF from the cytoplasmic side of the membrane—similar to the situation in vivo—strongly depends on the presence of LPS on the opposing side (Wiese et al. 1994).

During infection, components of the bacterial membranes are released into the environment due to the attack of the immune system or simply due to cell division. Since it is known that in particular membrane proteins and LPS form complexes, it can be assumed that these play a significant role also in the host, for example by interacting with immune cells such as human mononuclear cells leading to cell activation and induction of cytokines. It has been shown that LPS alone elicits a variety of biological reactions in mammals ranging from beneficial to pathological ones such as septic shock syndrome (Seydel et al. 1999). Thus, LPS is known to be one of the most potent stimuli of the immune system. Furthermore, it was found that porins may also stimulate cytokines such as interleukins and tumour necrosis factor α (Galdiero et al. 1993, 2001, 2002; Alurkar and Kamat 1997; Massari et al. 2002).

In the present paper, the interaction of OmpT with the membrane phospholipids and LPS—essential for its function in the bacterial outer membrane—is studied with infrared spectroscopy by investigating (1) the influence of the proteins on the gel to liquid-crystalline phase transition of the lipids—supplemented by some differential scanning calorimetric (DSC) experiments—and on vibrational bands in the interface (ester) and backbone (phosphate) region, and (2) the influence of the lipids on the secondary structure of the protein. Furthermore, the interaction of pure OmpT or LPS:OmpT complexes with phospholipid target cell membranes was studied with fluorescence resonance energy transfer spectroscopy (FRET). In biological assays, the ability of OmpT alone and in the presence of LPS to induce an inflammatory response (cytokine induction in human mononuclear cells) or a coagulation reaction (*Limulus* amoebocyte lysate assay), and the dependence of cell signaling on the Toll-like receptors TLR2 and 4 (CHO reporter system) were tested.

Materials and methods

Lipids and reagents

Lipopolysaccharide from the Ra mutants W3100 (K12) and DH5α from *Escherichia coli* and from the deep rough mutant Re of *Salmonella minnesota* (R595) were extracted by the phenol/chloroform/petrol ether method (Galanos et al. 1969) from bacteria grown at 37 °C, purified, and lyophilized. The chemical structures of the used LPS are shown in Fig. 1.

Bovine brain phosphatidylserine, egg phosphatidylcholine, phosphatidylethanolamine from *E. coli*, sphingomyelin from bovine brain, and the synthetic phospholipids dimyristoyl phosphatidylglycerol (DMPG) and dimyristoyl phospatidylethanolamine (DMPE) were purchased from Avanti Polar Lipids (Alabaster, AL, USA).

OmpT

OmpT was recombinantly expressed in *E. coli* and purified from inclusion bodies as described previously (Kramer et al. 2000, 2002) with some modifications.

Sample preparation

The lipid samples were usually prepared as aqueous dispersions (1–10 mM) for the phase-transition measurements (FTIR, DSC). Infrared measurements were performed in some cases also with hydrated samples, and measured at the instrument temperature of 28 °C. The lipids were suspended directly in HEPES buffer, sonicated and temperature-cycled several times between 5 and 70 °C and then stored at 4 °C for at least 12 h before measurement. For the elucidation of the protein secondary structure in the absence and presence of endotoxins, OmpT was prepared in buffer made either from H_2O or D_2O incubated at 37 °C for 0.5 h, and lipid dispersions prepared as described above were added in appropriate amounts, and further incubated at 37 °C for 15 min. Afterwards, 10 µl of these dispersions was spread on a CaF_2 infrared window, and the excess water was evaporated slowly at 37 °C.

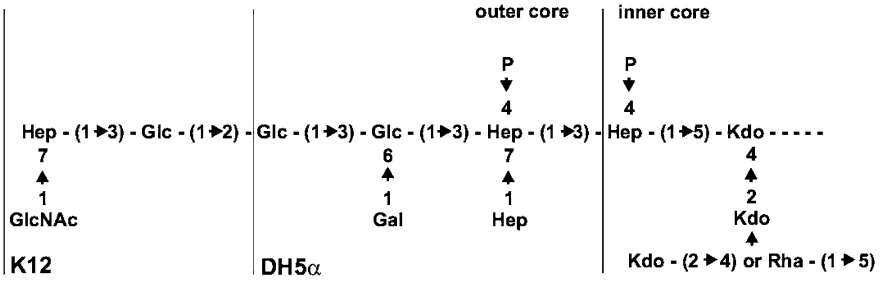

Fig. 1 Schematic core oligosaccharide structure of lipopolysaccharide from deep rough mutant Re (*Salmonella minnesota* R595) and from rough mutants Ra (*Escherichia coli* DH5α and K12). *Kdo* 2-Keto-3-deoxyoctonate, *Hep* L-*glycero*-D-*manno*-heptopyranose, *Rha* rhamnose, *Gal* galactose, *Glc* glucose

For preparation of liposomes from a phospholipid mixture corresponding to the composition of the cell membrane of macrophages—phosphatidylcholine, phosphatidylserine, phosphatidylethanolamine, and sphingomyelin in a molar ratio of 1:0.4:0.7:0.5 (Kröner et al. 1981), the lipids were solubilized in chloroform, and the solvent was evaporated under a stream of nitrogen. In a next step, the lipids were resuspended in the appropriate volume of buffer, and further treated as described for the lipids above.

For the analysis of the secondary structure of the protein via the analysis of the amide I band (predominantly C = O stretch) contour, aqueous protein solution was dispersed on a Ge crystal, and the excess water was slowly evaporated at room temperature. The sample was then placed in a closed cuvette and the air above the sample was saturated with water vapour.

FTIR spectroscopy

The infrared spectroscopic measurements were performed on a IFS-55 spectrometer (Bruker, Karlsruhe, Germany). For the phase-transition measurements via the analysis of the peak position of the symmetric stretching vibrational band of the methylene group around 2,850 cm^{-1}, the lipid samples were placed in a CaF_2 cuvette with a 12.5-μm Teflon spacer. Temperature scans were performed automatically between 10 and 70 °C with a heating rate of 0.6°C/min. Every 3 °C, 50 interferograms were accumulated, apodized, Fourier transformed, and converted to absorbance spectra. For secondary-structure determination (amide I band), hydrated samples were analysed to reduce the superimposed (OH-bending) water band. For strong absorption bands, the band parameters (peak position, band width, and intensity) were evaluated from the original spectra, if necessary after subtraction of the intensive water bands. The positions of the peak maxima were determined with a precision of better than 0.1 cm^{-1}. The infrared spectra were evaluated after base-line subtraction of neighbouring bands. In the case of overlapping bands, in particular for the analysis of the amide I vibration, curve fitting was applied using a modified version of the CURFIT program obtained by D. Moffat, NRC, Ottawa, Canada. An estimate of the number of band components was obtained from deconvolution of the spectra (Kauppinen et al. 1981), and the curve was fitted to the original spectra after subtraction of baselines resulting from neighbouring bands. The band shapes of the single components are superpositions of Gaussian and Lorentzian. Best fits were obtained by assuming a Gauss fraction of 0.55–0.60.

Differential scanning calorimetry (DSC)

A stock solution of 1 mg/ml of LPS Re was dispersed in 10 mM phosphate buffer at pH 6.8. LPS aggregates were obtained by sonication as described previously (Brandenburg et al. 2002b; Jürgens et al. 2002). A known amount of protein was added to the lipid dispersion at room temperature and the mixture slightly vortexed until full protein dissolution. Differential scanning calorimetry (DSC) measurements were performed with a MicroCal VP scanning calorimeter (MicroCal, Northhampton, MA, USA) at heating and cooling rates of 1 °C/min. Heating and cooling curves were measured in the temperature interval from 10–95 °C. Three consecutive heating and cooling scans were measured. For more details, see Blume and Garidel (1999).

Fluorescence resonance energy transfer (FRET) spectroscopy

The FRET assay was performed as described earlier (Schromm et al. 1996; Gutsmann et al. 2000). Briefly, phospholipid liposomes corresponding to the composition of the macrophage membrane ($PL_{M\phi}$) were doubly labeled with the fluorescent dyes *N*-(7-nitrobenz-2-oxa-1,3-diazol-4yl)-phosphatidylethanolamine (NBD-PE) and *N*-(lissamine rhodamine B sulfonyl)-phosphatidylethanolamine (Rh-PE) (Molecular Probes, Eugene, OR, USA). Intercalation of unlabeled molecules into the doubly labeled liposomes leads to probe dilution and with that to a lower FRET efficiency: the emission intensity of the donor at 531 nm increases and that of the acceptor at 593 nm decreases.

In all experiments, the protein OmpT was added after 50 s to the doubly labeled liposomes, and the FRET signal was monitored for at least 300 s. The resulting liposomes can be assumed to consist of a mixture of uni- and multilamellar liposomes. Therefore, only a qualitative estimate of a possible intercalation is possible.

Stimulation of human mononuclear cells (MNC)

For an examination of the cytokine-inducing capacity of the OmpT and LPS:OmpT mixtures, human mononuclear cells were stimulated with the latter and the TNFα production of the cells was determined in the supernatant.

MNC were isolated from heparinized (20 IU/ml) blood taken from healthy donors and processed directly by mixing with an equal volume of Hank's balanced solution and centrifugation on a Ficoll density gradient for 40 min (21 °C, 500 *g*). The interphase layer of mononuclear cells was collected and washed twice in Hank's medium and once in RPMI 1640 containing 2 mM L-glutamine, 100 U/ml penicillin, and 100 μg/ml streptomycin. The cells were resuspended in medium and the cell number was equilibrated at $5 \cong 10^6$ N/ml. For stimulation, 200 μl/well MNC ($5 \cong 10^6$ cells/ml) were transferred into 96-well culture plates. The stimuli were serially diluted in serum-free RPMI 1640 and added to

the cultures at 20 µl/well. The cultures were incubated for 4 h at 37 °C under 5% CO_2. Cell-free supernatants were collected after centrifugation of the culture plates for 10 min at 400 *g* and stored at −20 °C until determination of cytokine content.

Immunological determination of TNFα in the cell supernatant was performed in a sandwich ELISA as described elsewhere (Gallati 1982). A monoclonal (mouse) anti-human TNFα antibody (clone 16 from Intex AG, Switzerland) was used to coat the 96-well plates (Greiner, Solingen, Germany). Cell culture supernatants and the standard (recombinant human TNFα, Intex) were diluted with buffer. After exposure to appropriately diluted test samples and serial dilutions of standard rTNFα, the plates were exposed to peroxidase-conjugated (sheep) anti-mouse IgG antibody. Subsequently, the color reaction was started by addition of tetramethylbenzidine/H_2O_2 in alcoholic solution and stopped after 5–15 min by addition of 1 N sulfuric acid. In the color reaction, the substrate was cleaved enzymatically, and the product was measured photometrically on an ELISA plate reader at a wavelength of 450 nm, and the values were related to the standard. TNFα was determined in duplicate at two different dilutions and the values were averaged.

Determination of endotoxin activity by the chromogenic *Limulus* test

The biological activity of OmpT and LPS:OmpT mixtures at concentrations between 10 pg/ml and 10 µg/ml was also determined using a quantitative kinetic assay based on the reactivity of Gram-negative endotoxin with *Limulus* amoebocyte lysate (LAL) (Friberger et al. 1987), using test kits from LAL Coamatic Chromo-LAL K (Chromogenix, Haemochrom). The standard endotoxin used in this test was from *E. coli* (O113:H10) [endotoxin unit (EU)/ml corresponds to 1 ng/ml]. In this assay, saturation occurs at 125 EU/ml, and the resolution limit is ≤ 0.2 EU/ml (maximum value for ultrapure water from Sigma).

Cell lines

The possible involvement of the Toll-like receptors TLR-2 and TLR-4 in the cell activation by OmpT was investigated with the CHO reporter cell line, clone 3E10, which is stably transfected with human CD14 and expresses inducible human membrane CD25 (Tac antigen) under transcriptional control of the human E-selectin promoter (pELAM.Tac) (Delude et al. 1998). The chosen promoter fragment contains an essential nuclear factor NF-κB binding site (Yoshimura et al. 1999). The CHO/CD14/huTLR2 reporter cell line was constructed by stable cotransfection of 3E10 with the cDNA for human TLR2 as described (Delude et al. 1998). The CHO reporter cell line EL1 was obtained by stable transfection of CHO-K1 cells with pELAM.Tac. CHO cell lines were grown in Ham's F12 medium containing 10% FCS, 2 mM L-glutamine and 1% penicillin (100 U/ml)/streptomycin (100 µg/ml) at 37 °C in a humidified 5% CO_2 environment. Medium was supplemented with hygromycin B (400 U/ml) for 3E10 cells and hygromycin B (400 U/ml) plus G418 (0.5 mg/ml) for CD14/huTLR2 CHO cells.

Results

Since many of the presented data result from FTIR analyses, as an example one infrared spectrum of hydrated LPS from *Salmonella minnesota* strain R595 is shown (Fig. 2) in which the vibrational bands used for diagnosis are labelled as follows: (1) represents the symmetric stretching band of the methylene groups $\nu_s(CH_2)$ at 2,850 cm^{-1} as sensitive marker of the acyl-chain melting, (2) the ester carbonyl stretching vibration $\nu(C=O)$ around 1,730 cm^{-1}, (3) the phosphate antisymmetric stretching $\nu_{as}(PO_2^-)$ around 1,240 cm^{-1}, and (4) the amide I band around 1,650 cm^{-1} . The latter band, which here results from the two amide bindings in LPS (see Fig. 1) is expressed much more strongly in OmpT (data not shown), and was used for the analysis of the secondary structure of the protein.

Gel to liquid-crystalline phase transition

In the following, the acyl-chain melting induced by OmpT was studied for synthetic dimyristoyl phosphatidylethanolamine (DMPE) and phosphatidylglycerol

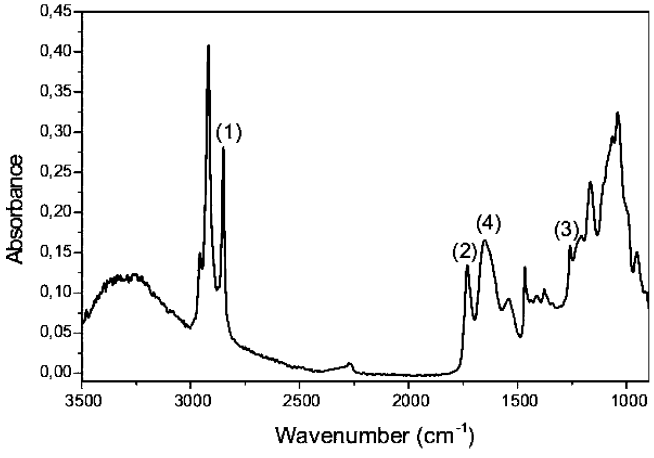

Fig. 2 Infrared spectrum of a hydrated LPS sample from *Salmonella minnesota* strain R595. The *labelled peaks* indicate the vibrational bands used for the analysis. *1*) Symmetric stretching vibration of the methylene groups, $\nu_s(CH_2)$; *2*) ester carbonyl stretching, $\nu(C=O)$; *3*) antisymmetric stretching of the negatively charged phosphate, $\nu_{as}(PO_2^-)$; *4*) amide I, predominantly C=O stretching, superimposed by water bending mode $\delta(OH)$

(DMPG) and for two LPS—deep rough mutant LPS Re from *Salmonella minnesota* strain R595 and the homologous LPS from DH5α from *Escherichia coli* (chemical structures see Fig. 1). The gel (β) to liquid-crystalline (α) phase transition of the hydrocarbon chains was monitored by analysing the peak position of $\nu_s(CH_2)$ as a function of temperature. The results in Fig. 3 for the two LPS and phospholipids exhibit—except for DMPE in the gel phase—a distinct fluidization of the acyl chains and a decrease in the phase-transition temperature T_c for all lipids due to the presence of OmpT, the former effect occurring already at very low OmpT concentrations ([lipid]:[OmpT] = 200:1 molar). In particular, for the two LPS preparations, the wavenumbers at 37 °C increased from values in the range 2,852.0–2,852.5 cm^{-1} to values around 2,853.7 cm^{-1}. For the phospholipids, in addition to the reduction in T_c, the values in the liquid-crystalline phase also shifted to wavenumbers 2,853.5–2,854.0 cm^{-1}.

Supplementary to the IR measurements, differential scanning calorimetry (DSC) was also applied to the LPS Re:OmpT system. Pure LPS Re showed a gel to liquid-crystalline phase transition at $T_c = 31$ °C ($T_{1/2} = 4.5$ °C) with $H_c = 38$ kJ/mol. The presence of OmpT induced a strong destabilization of the gel phase (Fig. 4). This was marked by strong broadening of the low-temperature side of the heat-capacity curve, with the peak maximum shifted by approximately 1 °C to lower temperature. At an LPS Re to OmpT molar ratio of 600:1, the peak half-width was $T_{1/2} = 8.2$ °C; thus, the coexistence range doubled as compared to the pure lipid. Increasing the amount of OmpT induced a slight increase in the peak width with a concomitant decrease in the phase-transition enthalpy. Compared to the phase-transition enthalpy of LPS Re, an H_c decrease of ~20% was measured for [LPS Re]:[OmpT] 100:1 (ΔH_c~30 kJ/mol). In the cooling scan of the system [LPS Re]:[OmpT] 100:1, a sharp exothermic peak at ~33.6 °C was observed with a large tailing on the low-temperature side of the heat-capacity curve (data not shown). During the first heating scan, the protein was denatured by heating up to 105 °C. Therefore, in the second heating scan, the interaction of LPS Re aggregates with denaturated OmpT was measured, which led to a gel-phase stabilization. Therefore, as expected, the second cooling scan was identical to the first one. Similar results were

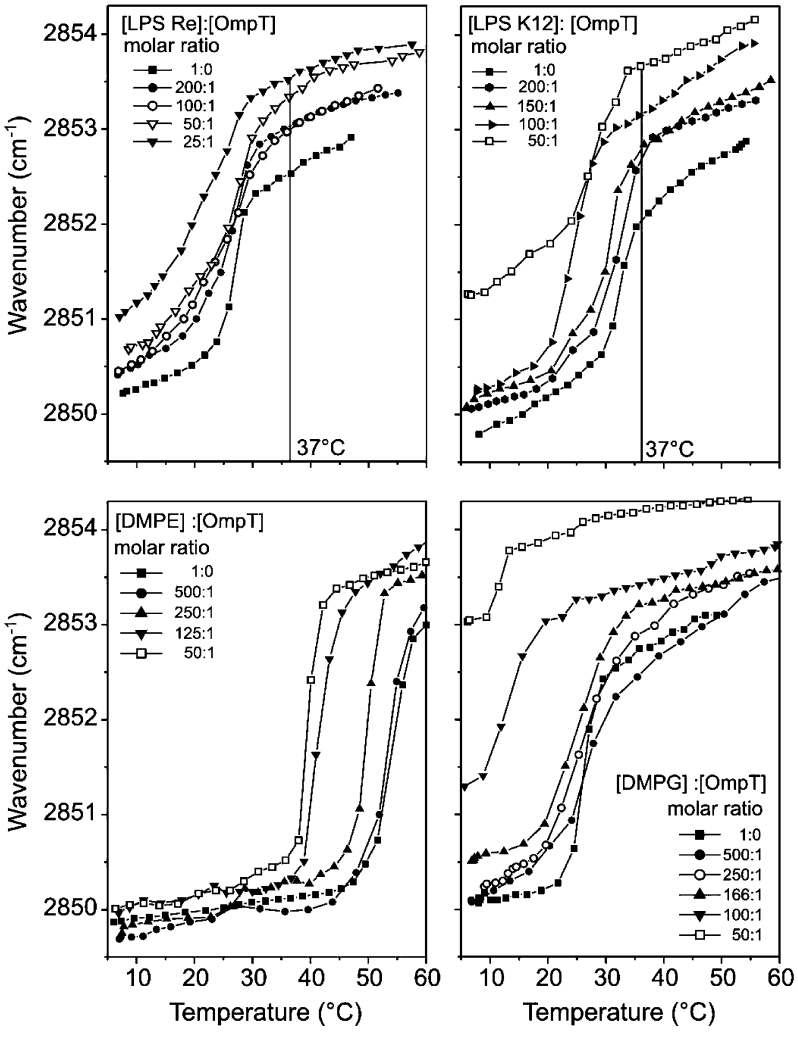

Fig. 3 Peak position of the symmetric stretching vibrational band $\nu_s(CH_2)$ versus temperature for different molar [*LPS*]:[*OmpT*], [*DMPE*]:[*OmpT*], and [*DMPG*]:[*OmpT*] ratios. In the gel (β) phase of the acyl chains, the typical peak position is around 2,849.5–2,850.5 cm^{-1}; in the liquid-crystalline (α) phase, it is located in the range 2,852.5–2,854 cm^{-1}

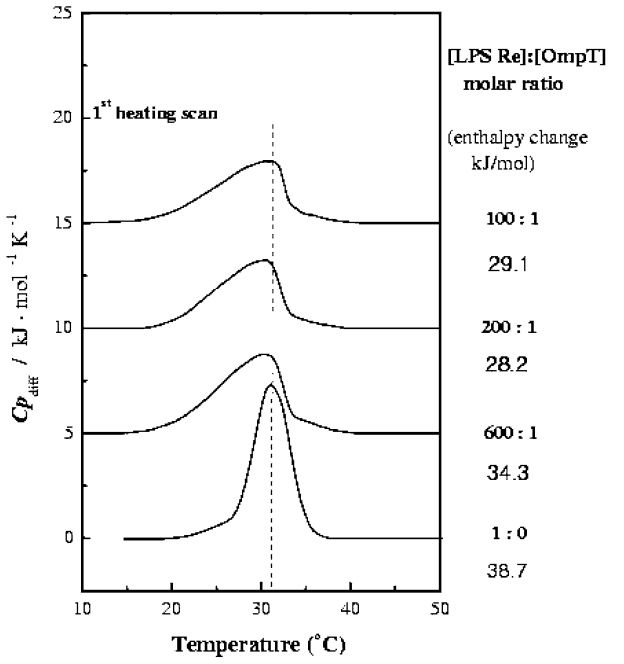

Fig. 4 Differential calorimetric scans of LPS Re (1 mg/ml) with varying concentrations of OmpT. The molar ratios are indicated in the *right margin*, as are the enthalpy changes corresponding to the areas of the endothermic transitions

obtained for the other investigated lipid to protein ratios (data not shown).

Binding of OmpT to LPS Re membranes provoked a strong perturbation of the organisation of the lipid hydrocarbon chains. The broadening of the low-temperature side of the DSC peak as well as a decrease in the phase-transition enthalpy is indicative of the reduction in the van der Waals interactions between the lipid acyl chains leading to increased hydrocarbon chain fluidity of the gel phase.

Ester band contour

The influence of the OmpT protein on the interface region of the lipids was characterized by studying the ester vibrational bands at 37 °C. The main ester vibrational band, predominantly due to C=O stretching, is located in the wavenumber range 1,760–1,700 cm^{-1}. This band contour usually consists of two band components around 1,740–1,730 cm^{-1} and around 1,720–1,710 cm^{-1} (sometimes also a third component around 1750 cm^{-1} is observed), independent of the number of ester groups within the molecules. The appearance of these different carbonyl absorption bands represents differently hydrated molecular groups with the band component at the lower wavenumber corresponding to higher hydration (Fringeli and Günthard 1981; Brandenburg 1993; Garidel et al. 2000). In Fig. 5 the wavenumber range 1,760–1,700 cm^{-1} is shown for different [LPS Re]:[OmpT], [DMPG]:[OmpT], and [DMPE]:[OmpT] molar ratios. For the phospholipids, the addition of OmpT clearly leads to an increase in band intensities but no wavenumber shift of the two main components, whereas in the case of LPS a change in the peak position with a shift to higher wavenumbers can also be observed. From these data, a considerable interaction of the phospholipids with OmpT leading to an increase in the mobility of the ester groups can be concluded. In contrast, the interaction of the ester groups of LPS Re with OmpT is

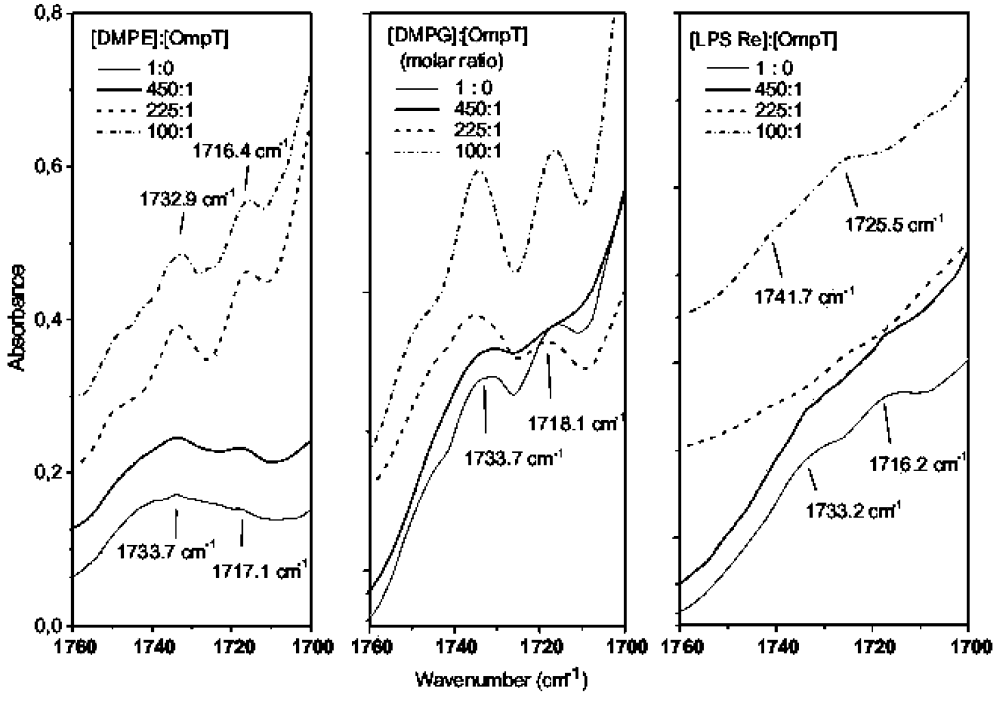

Fig. 5 Infrared spectra in the wavenumber region 1,760–1,700 cm^{-1} characteristic of the ester C=O band contour. The band components in the lower wavenumber range (1,720–1,710 cm^{-1}) correspond to highly hydrated ester groups, those in the higher wavenumber range (1,740–1,725 cm^{-1}) to less hydrated ester groups. For a better separation, different offset values were added to the baselines of the single curves

weak; only a slight dehydration ('blue' shift of the wavenumbers) can be seen.

Phosphate band contour of the lipids

The same spectra as presented above were analysed in the wavenumber range 1,320–1,180 cm^{-1} consisting of vibrational bands typical of the antisymmetric stretch of the negatively charged phosphate $\nu_{as}(PO_2^-)$ between 1,260–1,220 cm^{-1}, and in the case of LPS, the diglucosamine ring vibration at 1,180–1,160 cm^{-1}. Additionally, for gel-phase lipids, wagging progression bands may also be present in this spectral range. These weak bands, however, can be neglected here. From Fig. 6 it can be deduced that at least two phosphate band components in the range 1,280–1,200 cm^{-1} can be observed due to the existence of differently hydrated phosphate groups with the component at the higher wavenumber corresponding to a more dehydrated state (explicitly described for the system DMPG:Mg^{2+} by Garidel et al. 2000). Furthermore, it can be seen that the interaction of OmpT is much stronger with the phosphate groups of the phospholipids, in particular with those of DMPE, than with those of the two LPS. Thus, the strong band component at 1,220 cm^{-1} for DMPE was drastically reduced when increasing the OmpT concentrations (at [DMPE]:[OmpT] 166:1 molar, i.e. at a still low OmpT concentration). These data indicate an immobilization of the phosphate groups due to protein binding that is much less expressed for LPS than for the phospholipids. These observations relate to both lipopolysaccharides—LPS Re, which has two phosphates in the lipid A backbone, and LPS K12, which has an additional two

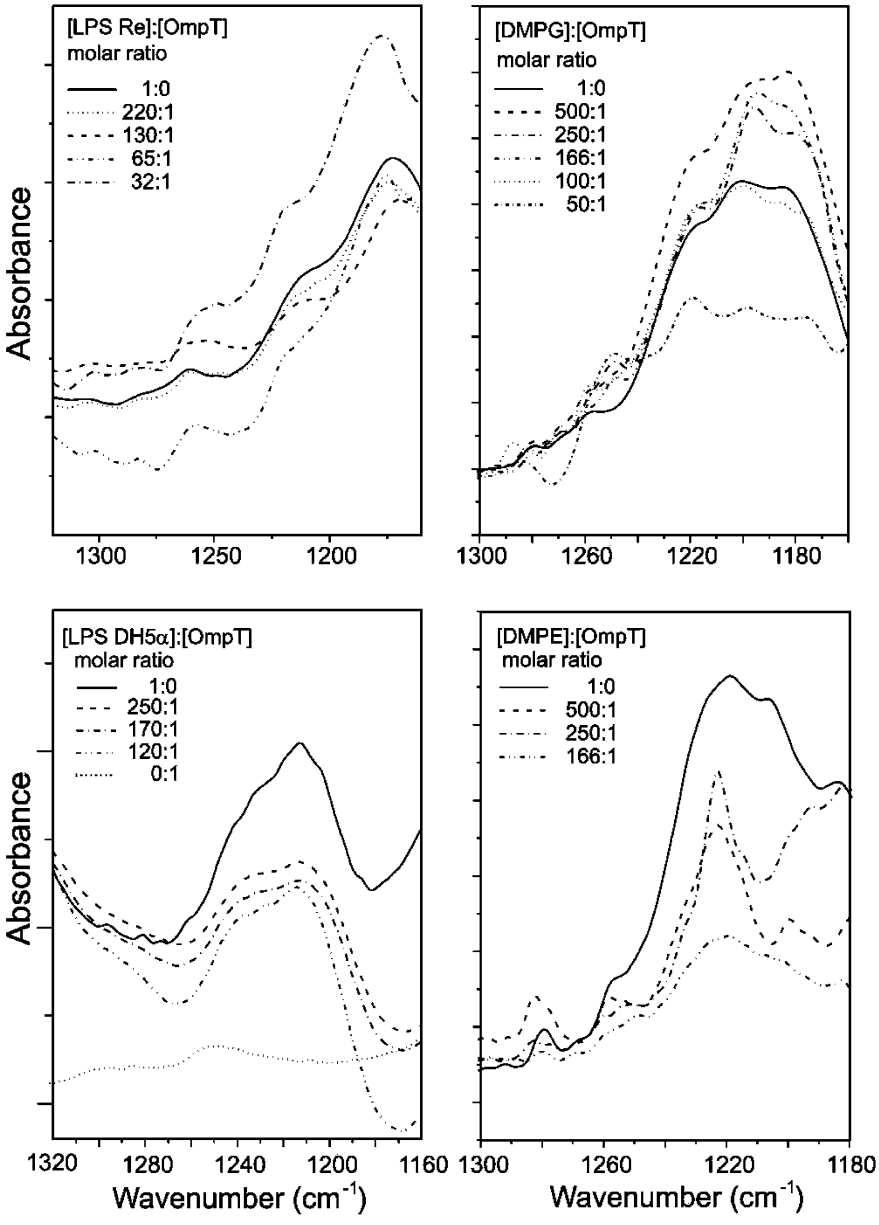

Fig. 6 Infrared spectra in the wavenumber region 1,300–1,180 cm^{-1} characteristic of the phosphate band contour. The band components in the lower wavenumber range (1,230–1,210 cm^{-1}) correspond to highly hydrated phosphate groups, those in the higher wavenumber range (1,270–1,240 cm^{-1}) to less hydrated phosphate groups

phosphates in the heptose region, i.e. four phosphate groups. Whereas the broad band contour of LPS K12 indicates the existence of a variety of hydration states, LPS Re has two single band components at 1,220 and 1,260 cm^{-1} corresponding to the two differently hydrated phosphates, with the 1-phosphate sticking into the aqueous phase and the 4′-phosphate buried in the membrane (Seydel et al. 2000).

Secondary structure of OmpT

The analysis of the secondary structure of OmpT in the absence and presence of the different lipids was done by evaluating the IR spectrum of hydrated samples in the range of the amide I vibrational band, which shows a complex splitting into single components according to the water-binding capability of the secondary structures (Arrondo and Goni 1999). Thus, the characteristic secondary structures for α-helical structures are in the range 1,658–1,650 cm^{-1}, and β-sheet structures have the main peak in the range 1,635–1,628 cm^{-1}, and may have additional ones around 1,620 cm^{-1} (intermolecular aggregated forms) and 1,685–1,670 cm^{-1} (β turns and antiparallel β sheets). Random-coil (unordered) structures lie in the range 1,665–1,658 cm^{-1}, which is shifted to 1,645–1,640 cm^{-1} if D_2O instead of H_2O is used in the buffer. We made measurements in both solvents to avoid a possible misinterpretation of the α-helical and unordered structures, but also to avoid errors due to the superimposed water bending band at 1,645 cm^{-1}.

Figure 7a shows the infrared spectrum of OmpT in the amide I region at two different water concentrations (excess water and hydrated) including a curve-fit analysis. Clearly, the data indicate the occurrence of β-sheet as well as α-helical structures, and a weak dependence on water content, i.e. a higher number of β sheets when the water content is reduced. The corresponding spectra in the presence of the lipids are given in Fig. 7b showing clearly a dramatic increase in the number of β-sheet structures of the protein in the presence of all lipids. All data of the secondary-structure determination are summarized in Tables 1 and 2. In Table 1, the mean values of the secondary structures of differently hydrated OmpTs are given, showing the dominance of β structures, but also the presence of α-helical structures to a significant degree. It should be noted that the measurements in D_2O led to the same results, in particular, the α-helical structures cannot be misinterpreted as resulting from unordered structures. As a control, OmpT was boiled for 0.5 h, which should destroy the highly ordered α-structures. This is actually the case essentially in favour of intermolecular β aggregates and unordered structures (Table 1). In a similar way, in DSC measurements the excess heat-capacity versus temperature curve showed a drastic decrease at temperatures slightly above 100 °C, and a straight line in the second scan which was interpreted to be due to denaturation and aggregation processes (data not shown). The results of

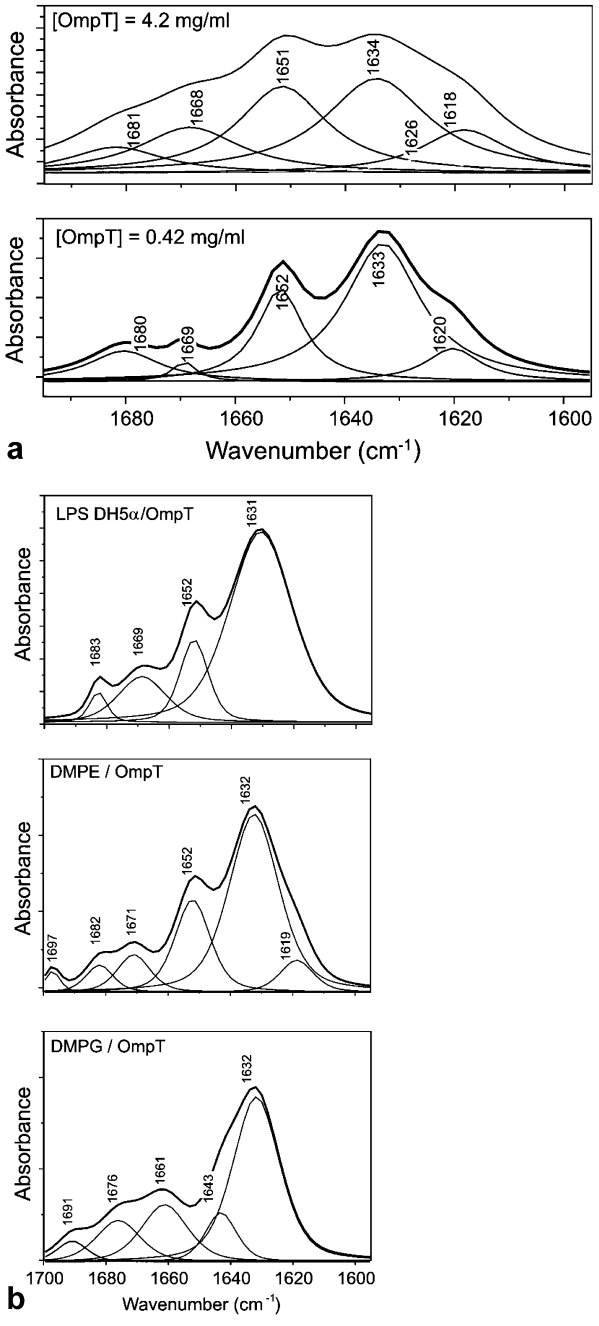

Fig. 7 Infrared spectra in the range 1,700–1,590 cm^{-1} characteristic of the amide I vibrational band (predominantly C = O) for pure *OmpT* at different concentrations (**a**) and for *LPS-*, *DMPE-*, and *DMPG-OmpT* mixtures in a concentration range [lipid]:[OmpT] = 100:1 molar (**b**). The main band component around 1,640–1,625 cm^{-1} is characteristic of β-sheet structures, that around 1,655–1,650 cm^{-1} of α-helical structures (Arrondo and Goni 1999). Further band components around 1,620–1,615 cm^{-1} correspond to intermolecular aggregates and around 1,685–1,670 cm^{-1} to β turns and antiparallel β sheets. The temperature was 28 °C

the binding measurements of OmpT with LPS K12 and with DMPG and DMPE (Table 2) showed an increase in the number of β-sheet structures and a decrease in α-helical structures. For LPS K12, this increase was strong

Table 1 Relative number of secondary structures of pure OmpT from infrared spectra in the range of the amide I vibration (1,700–1,590 cm^{-1}) deduced from the determination of the band areas after curve fitting as shown in Fig. 6a

Secondary structure	OmpT in excess buffer	OmpT hydrated	OmpT mean value ($n=6$)	OmpT boiled
α Helix	27	22	26 ± 2	0
β Sheet	35	54	45 ± 9	0
β Turns	16	2	9 ± 6	13
Bintermolecular	13	9	14 ± 3	40
β Antiparallel	9	12	6 ± 3	0
Unordered	0	0	0	43
Not assignable	0	1	0	4

Table 2 Relative number of secondary structures of OmpT after binding to LPS and to the phospholipids DMPE and DMPG, from infrared spectra in the range of the amide I vibration (1700–1590 cm^{-1}), deduced from the determination of the band areas after curve fitting as shown in Fig. 6b. The error margin can be estimated at ±3%

Secondary structure	LPS K12				DMPG			DMPE	
	DH5α/OmpT	OmpT							
	30:1 molar I	5:1 molar Batch 1	1:1 molar	5:1 molar Batch 2	4:1 molar	2:1 molar	1:1 molar	3:1 molar	1:1 molar
α Helix	7	15	8	13	0	0	0	22	17
β Sheet	81	49	58	56	51	54	55	57	56
β Turns	8	7	11	7	21	2	15	8	16
β Intermolecular	0	0	10	24	0	0	0	2	6
β Antiparallel	2	29	3	0	0	0	0	5	5
Unordered	0	0	0	0	13	18	24	0	0

at a very high molar excess of LPS (30:1 molar). Furthermore, the interaction of PG with OmpT led to a complete disappearance of α-helical structures, whereas for LPS K12 a reduction took place. In contrast, the zwitterionic lipid PE changed the secondary structure of OmpT only very slightly as compared to the pure protein.

In the case of LPS, the results were similar for the three different Ra-type endotoxins (two batches LPS K12 W3100 and one batch LPS DH5α) except for one sample in which the proteins also exhibited intermolecular sheets. Interestingly, PG bound to OmpT in a way that all α-helical structures disappeared in favour of the occurrence of unordered structures.

Incorporation into target membranes

It is conceivable that the OmpT protein as membrane protein could not only intercalate into outer membranes, but also into the membranes of host cells such as the macrophages. This could lead to strong membrane disturbance with possible subsequent cell activation. Thus, using FRET spectroscopy, the ability of OmpT to intercalate into phospholipid liposomes corresponding to the composition of macrophage membranes was investigated. When OmpT was added to the liposomes, the fluorescence signal of the donor dye emission showed a decrease in intensity corresponding to a dilution of the liposome dispersion. This indicated that no incorporation of the protein into the liposomes took place (data not shown). This was found to hold true for very high OmpT concentrations up to an equimolar range of phospholipid and OmpT and also true when the phospholipid liposomes were made from negatively charged phosphatidylserine.

Biological activity

Since it is known that proteins such as OmpT usually are released from the outer membrane complexed with LPS and, furthermore, that membrane proteins such as porins may exert biological activity by themselves, the ability of OmpT as well as LPS:OmpT mixtures to (1) induce the production of tumour-necrosis-factor α (TNFα) in human mononuclear cells (MNC) and (2) react in the *Limulus* amoebocyte lysate (LAL) assay was investigated. In Fig. 8, the TNFα production of human MNC induced by different concentrations of OmpT is shown. Clearly, a concentration-dependent increase in the cytokine production is observed. To test the possibility that an LPS contamination was responsible for this observation, pure LPS Re, pure OmpT, and LPS Re/OmpT mixtures were investigated with respect to their cytokine induction. The results are given in Fig. 9. Apparently, the OmpT did not contain a significant contamination of LPS Re but induced cytokines by itself, since the addition of 4.2 μg/ml or 420 ng/ml OmpT to 100 ng/ml LPS Re (Fig. 9, above) caused a reduction in the cytokine induction, which was similarly true for the lower concentrations as presented in Fig. 9, below.

The comparison of the TNFα-inducing capacity of OmpT (100 ng/ml) before and after boiling showed a

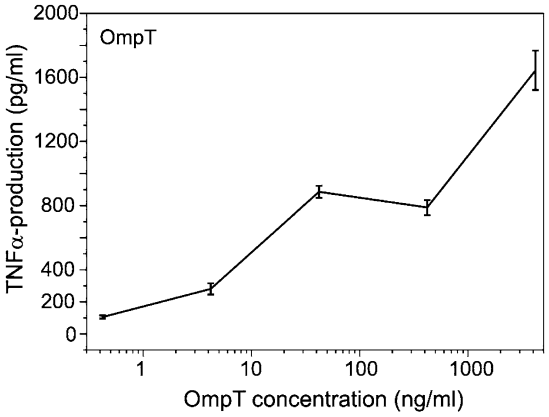

Fig. 8 Production of tumour-necrosis-factor α (*TNFα*) by human mononuclear cells induced by different concentrations of *OmpT*. The *error bars* (standard deviation) result from the determination of TNFα in duplicate at two different dilutions. The data are representative of three independent experiments

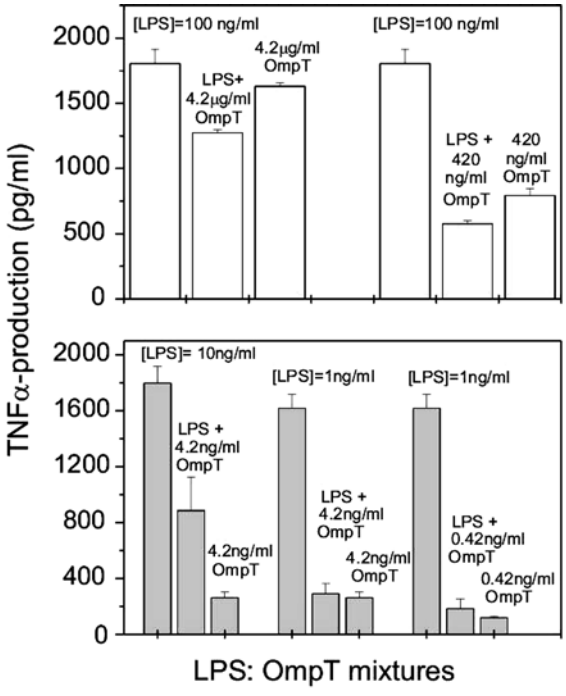

Fig. 9 Production of tumour-necrosis-factor α (*TNFα*) by human mononuclear cells induced by different concentrations of *OmpT*, *LPS Re*, and *LPS-OmpT* mixtures. The *error bars* (standard deviation) result from the determination of TNFα in duplicate at two different dilutions. The data are representative of three independent experiments

decrease from 650 to 250 pg/ml TNFα concentration. The residual activity may be indicative of some LPS contamination. This was confirmed by applying the LAL assay, which is specific for LPS and does not react with proteins. As summarized in Table 3, the increase in the OmpT values before and after boiling indicate the presence of LPS, which was possibly not detectable by this assay before boiling due to hidden binding groups of LPS. By comparing these data with the values for pure LPS, the LPS content within the OmpT, preparation can be estimated to be around 2 pg/ml.

Dependence of signalling on Toll-like receptors 2 and 4

Toll-like receptors (TLR) have been described as a family of cellular receptors critically involved in cell activation by a variety of bacterial virulence factors. Thus, TLR4 has been identified to be responsible for cell activation by bacterial LPS (Beutler 2000), whereas TLR2 is involved in cell activation of bacterial compounds such as peptidoglycan, lipopeptides, and lipoteichoic acid (Yoshimura et al. 1999). To investigate the potential involvement of TLR2 and TLR4 in the recognition of OmpT, we employed Chinese hamster ovary (CHO) reporter cells expressing the human proteins CD14, TLR2, or TLR4 (Delude et al. 1998). These cells are stably transfected with an NF-κB-dependent reporter gene, driving the gene for human Tag antigen, which is expressed on the cell surface upon cell activation (Heine et al. 1999). These cells were used in stimulation experiments with OmpT. Neither the TLR2- nor the TLR4-expressing cell line was activated by OmpT, but by the internal controls (synthetic lipopeptide Pam_3CSK_4 activated CD14.TLR2 CHO cells and LPS activated CD14.TLR4 CHO cells, data not shown). These results suggest that neither TLR2 nor TLR4 is involved in cell activation by OmpT. Furthermore, the biological activity of OmpT preparations was not due to contaminations with LPS or lipopeptides, since these would naturally lead to an activation of CD14.TLR2 or CD14.TLR4 CHO cells.

Discussion

The study of the interaction of OmpT with the outer-membrane constituents PE, PG, and LPS clearly proves a very tight binding of the protein with the main lipid compounds in all cases—except for DMPE in the gel

Table 3 Activity of some LPS and OmpT preparations in endotoxin units (EU)/ml in the *Limulus*amoebocyte lysate test (for standard endotoxin from *E.coli* O55:B5, 10 EU/ml corresponds to 1 ng/ml)

	LPS Re (1 ng/ml)	LPS Re (10 ng/ml)	OmpT (28 µg/ml)	OmpT (28 µg/ml, boiled)	H_2O
EU/ml	45.6	>126	0.13	1.04	0.02

phase—leading to a strong fluidization of the acyl chains of the lipids. Although our studies do not include experiments with the native outer membrane, the data indicate that the presence of OmpT should also reduce the acyl-chain order within the asymmetric bilayer of the outer membrane. This fluidization starts at a very high lipid:OmpT molar ratio and thus should be physiologically relevant. It can be assumed that at the lowest OmpT concentrations at which fluidization was observed (Fig. 3) not all lipid molecules were affected, but probably only those in close vicinity to the protein. A more detailed description of this phase separation, however, is not possible, since the FTIR signal is an average over all lipid molecules.

These data can explain the observations that the outer membrane is very stable despite the fact that one layer (LPS) is present in a very highly ordered state—much less fluid than phospholipids (Labischinski et al. 1985)—and that even a considerable decrease in growth temperature of bacteria changes the chemical structure of LPS only slightly in contrast to the observations for phospholipids. Thus, when the growth temperature was reduced from 37 to 22 °C, a 16:1 fatty acid was synthesized at the expense of one of the 3-OH fatty acids of LPS, which led to a reduction in T_c from 30 to 25 °C, i.e. above the growth temperature (Brandenburg and Blume 1987). In contrast, the change in the growth temperature led to a much greater change in the chemical structure of the phospholipids (Lindner and Seydel 1984). In accordance with the 'high state of order of LPS' (Labischinski et al. 1985) it has been published that the outer membrane represents a high permeability barrier in particular against large hydrophobic drugs due to the existence of the LPS outer leaflet, especially the highly ordered hydrocarbon moiety (Nikaido 1993; Snyder and McIntosh 2000). These properties may hold true for the pure lipid matrix, but our data in the presence of OmpT do not indicate a significantly higher order of the LPS as compared to that of the phospholipids. Regarding the barrier property, it seems to be much more probable that the extremely hydrophilic sugar head group of LPS may be responsible for this. Therefore, one main role of integral membrane proteins such as OmpT seems to be levelling the existing acyl-chain mobility gradients between the two leaflets of the outer membrane.

The finding in accordance with the IR spectroscopic data from Fig. 3 and the DSC data indicating a gel-phase destabilization of LPS and a decrease in the lipid T_c (Fig. 4) is in contrast to what was found for the interaction of LPS with the natural antibiotics lysozyme and lactoferrin (Brandenburg et al. 1998, 2001), hemoglobin from red blood cells (Jürgens et al. 2001), and the serum proteins high-density lipoprotein (HDL; Brandenburg et al. 2002a) and (recombinant) albumin (Jürgens et al. 2002). For all these non-membrane proteins, a gel-phase stabilization connected with an increase in T_c takes place. Thus, this basic difference may reflect completely different functions of the various proteins. Very importantly, the strong fluidization of the LPS acyl chains is not a singular property of OmpT; we have found that porins from the bacterial outer membrane also induce a similar effect at very low protein concentrations (own unpublished data in collaboration with W. Welte, Universität Konstanz).

The results obtained from the analysis of the phosphate and ester vibrations (Figs. 5, 6) indicate a stronger interaction of OmpT with the phospholipid head groups of PE and PG than with the LPS backbone. The binding of OmpT led to rigidified phosphates but more fluid ester groups of the phospholipids, and together with the phase-transition data, the action of OmpT on the inner layer of the outer membrane consisted of a rigidification of the lipid head groups and fluidization in the interface and hydrophobic region. The action of OmpT on the outer LPS layer consisted only of a fluidization of the acyl chains, i.e. there is only a weak interaction with the LPS backbone. This behaviour may reflect an asymmetric location of OmpT, with a preference for the phospholipid side, or a directed intercalation of OmpT in the asymmetric outer membrane, which seems to be connected with its function.

The fluidizing role of OmpT seems also to be important with respect to the outer-membrane stability. The phase-transition temperature T_c of pure enterobacterial LPS was found to lie close to the physiological temperature (see Fig. 3), in particular for various smooth form LPS even at temperatures >37 °C (Brandenburg and Blume 1987). It is currently accepted, however, and has also been experimentally verified with a planar asymmetric membrane system (Hagge et al., unpublished results), that such membranes are too unstable.

Noteworthy are the data from the secondary-structure determination of OmpT (Fig. 7 and Table 2) that emphasize the importance of the water content to the interpretation of the spectra. Besides the dominant β-sheet structure in accordance with the study by Kramer et al. (2000) applying CD spectroscopy, α-helical structures were also observed, which seemed to be expressed most strongly at higher water content (Table 1), but are reduced in the presence of lipids. These data seem to be in contradiction to Vandeputte-Rutten et al. (2001), who found β-sheet structures for crystallized OmpT 69% , but no α-helical structures (see also Protein Data Bank, no. 1I78). However, it has to be considered that the relatively high water content applied here may play a role. It has been shown that the 'solution' structure of the protein α-lactalbumin deduced from CD and FTIR spectroscopy dramatically differed from the crystal structure as determined by X-ray crystallography (Urbanova et al. 1991) in that the protein solution structure had fewer helical (α- and 3_{10}-) structures than the protein crystal. In this context, the decrease in the α-helical structures with decreasing water content (Table 1) may be understood. Our data are in rough accordance with those of Kramer et al. (2002) who found no large structural changes of OmpT secondary structure on addition of LPS. This was surprising since

the protease activity of OmpT was only obtained after addition of LPS. For this activity, only a subtle conformational change, caused by LPS binding, seems to be necessary.

The data of the cytokine induction in human mononuclear cells induced by OmpT (Fig. 8) and LPS:OmpT mixtures (Fig. 9) indicate a strong capacity of the protein to induce TNFα production. The contamination of OmpT with LPS is by far not high enough—considering the results from the experiments with the boiled protein in the *Limulus* assay—to explain this potency. Furthermore, the addition of corresponding concentrations of LPS, which alone led to a high signal, reduced the TNFα-inducing capacity of pure OmpT (see Fig. 9, above). The results in Fig. 9 for the mixtures are interesting: the addition of OmpT to LPS Re at the given concentrations in all cases led to a decrease in LPS Re immunostimulatory activity which might be explained by the fact that the binding sites in LPS Re for serum and membrane proteins such as LBP and CD14 are partially hidden or occupied. Concomitantly, or as an alternative model, it is also possible that the LPS aggregate structure is stabilized by binding to OmpT which would increase the binding energy of the LPS molecules within the aggregate. This would run parallel to the action of the polycationic decapeptide polymyxin B (PMB), which also led to a strong fluidization of the lipid A acyl chains of LPS (Brandenburg et al. 2002b) and an increase in the binding energy for lipid A aggregates from −490 meV (-7.8×10^{-20} J) to more than −570 meV (Buschner 1999).

The capacity of OmpT to induce cytokines such as TNFα in mononuclear cells is not a result of the incorporation of the protein into the membrane of these cells, since the FRET data did not show any signal characteristic of this process. To the best of our knowledge, it has never been reported that OmpT proteins may induce cytokines. However, in the literature there are some reports about biological activity of other Omp molecules, the porins. Galdiero et al. (1993) were the first authors to describe porin-induced cytokine production in human cells. They found the release of TNFα, IL-1, and IL-6 by human monocytes and of γ-interferon and IL-4 by lymphocytes when exposed to porins from rough mutant and wild-type strains from *Salmonella thyphimurium*. Analogously, Alurkar and Kamat (1997) studied the immunomodulatory properties of some porins from enterobacteria and found, among others, an IL-1 induction in peritoneal cells from mice. Very recently, a more detailed study by Galdiero and coworkers (2001) found cytokine (IL-6, IL-8, and TNFα) production in the human monocyte cell line THP-1 induced by a porin concentration as low as 50 ng/ml. Furthermore, neither the presence of serum nor CD14 influenced this activity, only the presence of the integrins CD11a/CD18 exhibited a slight influence. Investigations into the early responses after porin stimulation showed that the cell-signalling pathways include activating protein 1 (AP1) and nuclear factor κB (NF-κB) through the mitogen-activated protein kinase (MAPK) cascade (Galdiero et al. 2002). The authors found differences in the signalling by LPS because the cytokine release after stimulation with porins began after 2 h and lasted for 5–6 h, whereas the release after LPS stimulation started after 30 min and decreased after 2 h. The authors also tested the porin preparations for LPS contamination by applying the *Limulus* test as well as polymyxin B to remove LPS, but found no evidence for a contamination. Massari et al. (2002) found stimulation of murine B cells by *Neisseria* porins to be dependent on TLR2 and the adapter protein MyD88, which was deduced from the lack of response in TLR2- and MyD88-knockout mice.

The present data from the CD25 reporter cell line clearly indicate that neither the Toll-like receptor TLR4, which is usually responsible for LPS signalling (Beutler 2000), is involved, nor TLR2, which has been observed to play a role in the case of lipopeptides and lipoproteins and also for particular proteins such as hemagglutinin from measles virus (Bieback et al. 2002; Morr et al. 2002). These data are furthermore indicative that the biological activity observed was not due to a contamination of LPS. An identification of the cellular receptors responsible for cell activation by OmpT will be an important step in understanding the pathobiological mechanisms underlying the release of bacterial membrane proteins.

In summary, our observations emphasize the role of bacterial membrane proteins in the inflammatory host response, since the release of Omp:LPS complexes from the outer membrane can be assumed to be the rule rather than an exception.

Acknowledgements We are indebted to G. von Busse and C. Hamann for performing the IR spectroscopic and fluorescence spectroscopic measurements. The expert help of B. Fölting for performing the DSC and U. Diemer, the LAL measurements, is kindly acknowledged. This work was financially supported by the Commission of the European Communities, specific RTD programme Quality of Life and Management of Living Resources, QLK-CT-2002-01001, "Antimicrobial endotoxin neutralizing peptides to combat infectious diseases".

References

Alurkar V, Kamat R (1997) Immunomodulatory properties of porins of some members of the family *Enterobacteriaceae*. Infect Immun 65:2382–2388

Arrondo JL, Goni FM (1999) Structure and dynamics of membrane proteins as studied by infrared spectroscopy. Prog Biophys Mol Biol 72:367–405

Beutler B (2000) Endotoxin, Toll-like receptor 4, and the afferent limb of innate immunity. Curr Opin Microbiol 3:23–28

Bieback K, Lien E, Klagge IM, Avota E, Schneider-Schaulies J, Duprex WP, Wagner H, Kirschning CJ, ter Meulen V, Schneider-Schaulies S (2002) Hemagglutinin protein of wild-type measles virus activates Toll-like receptor 2 signaling. J Virol 76:8729–8736

Blume A, Garidel P (1999) Lipid model membranes and biomembranes. In: Gallagher PK, Kemp RB (eds) The handbook of thermal analysis and calorimetry. Elsevier, Amsterdam, pp 109–173

Brandenburg K (1993) Fourier transform infrared spectroscopy characterization of the lamellar and nonlamellar structures of free lipid A and Re lipopolysaccharides from *Salmonella minnesota* and *Escherichia coli*. Biophys J 64:1215–1231

Brandenburg K, Blume A (1987) Investigations into the thermotropic phase behaviour of natural membranes extracted from Gram-negative bacteria and artificial membrane systems made from lipopolysaccharides and free lipid A. Thermochim Acta 119:127–142

Brandenburg K, Koch MHJ, Seydel U (1998) Biophysical characterisation of lysozyme binding to LPS Re and lipid A. Eur J Biochem 258:686–695

Brandenburg K, Jürgens G, Müller M, Fukuoka S, Koch MHJ (2001) Biophysical characterization of lipopolysaccharide and lipid A inactivation by lactoferrin. Biol Chem 382:1215–1225

Brandenburg K, Jürgens G, Andrä J, Lindner B, Koch MHJ, Blume A, Garidel P (2002) Biophysical characterization of the interaction of high-density lipoprotein (HDL) with endotoxins. Eur J Biochem 269:5972–5981

Brandenburg K, Moriyon I, Arraiza MD, Lehwark-Yvetot G, Koch MHJ, Seydel U (2002) Biophysical investigations into the interaction of lipopolysaccharide with polymyxins. Thermochim Acta 382:189–198

Buschner S. (1999) Bestimmung der kritischen Aggregatkonzentration von Lipiden: Implikationen für die biologische Wirksamkeit von Endotoxinen. PhD Thesis, Universität Kiel

Dekker N, Cox RC, Kramer RA, Egmond MR (2001) Substrate specificity of the integral membrane protease OmpT determined by spatially addressed peptide libraries. Biochemistry 40:1694–1701

Delude RL, Yoshimura A, Ingalls RR, Golenbock DT (1998) Construction of a lipopolysaccharide receptor cell line and its use in identifying mutants defective in endotoxin, but not TNFα, signal transduction. J Immunol 161:3001–3009

Friberger P, Sörskog L, Nilsson K, Knös M (1987) The use of a quantitative assay in endotoxin testing. In: Watson SW, Levin J, Novitzky TJ (eds) Detection of bacterial endotoxin with the limulus amebocyte lysate test. Alan Liss, New York, pp 149–169

Fringeli UP, Günthard HH (1981) Infrared membrane spectroscopy. In: Grell E (ed) Membrane spectroscopy. Springer, Berlin New York, pp 270–332

Galanos C, Lüderitz O, Westphal O (1969) A new method for the extraction of R lipopolysaccharides. Eur J Biochem 9:245–249

Galdiero F, Cipollardo de L'Ero G, Benedetto N, Galdiero M, Tufano MA (1993) Release of cytokines induced by *Salmonella typhimurium* porins. Infect Immun 61:155–161

Galdiero M, D'Isanto M, Vitiello M, Finamore E, Peluso L (2001) Porins from *Salmonella enterica* serovar Typhimurium induce TNF-alpha, IL-6 and IL-8 release by CD14-independent and CD11a/CD18-dependent mechanisms. Microbiology 147:2697–2704

Galdiero M, Vitiello M, Sanzari E, D'Isanto M, Tortora A, Longanella A, Galdiero S (2002) Porins from *Salmonella enterica* Serovar Typhimurium activate the transcription factors activating protein 1 and NF-kappaB through the Raf-1 mitogen activated protein kinase cascade. Infect Immun 70:558–568

Gallati H (1982) Interferon: Wesentlich vereinfachte, enzym-immunologische Bestimmung mit zwei monoklonalen Antikörpern. J Clin Chem Clin Biochem 20:907–914

Garidel P, Blume A, Hübner W (2000) A Fourier transform infrared spectroscopic study of the interaction of alkaline earth cations with the negatively charged phospholipid 1,2-dimyristoyl-*sn*-glycero-3-phosphoglycerol. Biochim Biophys Acta 1466:245–259

Gutsmann T, Schromm AB, Koch MHJ, Kusumoto S, Fukase K, Oikawa M, Seydel U, Brandenburg K (2000) Lipopolysaccharide-binding protein-mediated interaction of lipid A from different origin with phospholipid membranes. Phys Chem Chem Phys 2:4521–4528

Heine H, Kirschning CJ, Lien E, Monks BG, Rothe M, Golenbock DT (1999) Cutting edge: cells that carry a null allele for Toll-like receptor 2 are capable of responding to endotoxin. J Immunol 162:6971–6975

Jürgens G, Müller M, Koch MH J, Brandenburg K (2001) Interaction of hemoglobin with enterobacterial lipopolysaccharide and lipid A. Physicochemical characterization and biological activity. Eur J Biochem 268:4233–4242

Jürgens G, Müller M, Garidel P, Koch MHJ, Nakakubo H, Blume A, Brandenburg K (2002) Investigation into the interaction of recombinant human serum albumin with Re-lipopolysaccharide and lipid A. J Endotoxin Res 8:115–126

Kauppinen JK, Moffat DJ, Mantsch HH, Cameron DG (1981) Fourier self-deconvolution: a method for resolving intrinsically overlapped bands. Appl Spectrosc 35:271–276

Kramer RA, Zandwijken D, Egmond MR, Dekker N (2000) In vitro folding, purification and characterization of *Escherichia coli* outer membrane protease OmpT. Eur J Biochem 267:885–893

Kramer RA, Vandeputte-Rutten L, de Roon GJ, Gros P, Dekker N, Egmond MR (2001) Identification of essential acidic residues of outer membrane protease OmpT supports a novel active site. FEBS Lett 505:426–430

Kramer RA, Brandenburg K, Vandeputte-Rutten L, Werkhoven M, Gros P, Dekker N, Egmond MR (2002) Lipopolysaccharide regions involved in the activation of *Escherichia coli* outer membrane protease OmpT. Eur J Biochem 269:1746–1752

Kröner EE, Peskar BA, Fischer H, Ferber E (1981) Control of arachidonic acid accumulation in bone marrow-derived macrophages by acyltransferases. J Biol Chem 256:3690–3697

Labischinski H, Barnickel G, Bradaczek H, Naumann D, Rietschel ET, Giesbrecht P (1985) High state of order of isolated bacterial lipopolysaccharide and its possible contribution to the permeation barrier of the outer membrane. J Bacteriol 162:9-20

Lindner B, Seydel U (1984) Laser Mikrosonden Massenanalyse (LAMMA) in der Mikrobiologie. Forum Mikrobiol 7:332–338

Massari P, Henneke P, Ho Y, Latz E, Golenbock DT, Wetzler LM (2002) Cutting edge: immune stimulation by neisserial porins is Toll-like receptor 2 and MyD88 dependent. J Immunol 168:1533–1537

Morr M, Takeuchi O, Akira S, Simon MM, Mühlradt PF (2002) Differential recognition of structural details of bacterial lipopeptides by Toll-like receptors. Eur J Immunol 32:3337–3347

Nikaido H (1993) Transport across the bacterial outer membrane. J Bioenerg Biomembr 25:581–589

Nikaido H, Vaara,M (1985) Molecular basis of bacterial outer membrane permeability. Microbial Rev 49:1–32

Schromm AB, Brandenburg K, Rietschel ET, Flad H-D, Carroll SF, Seydel U (1996) Lipopolysaccharide binding protein (LBP) mediates CD14-independent intercalation of lipopolysaccharide into phospholipid membranes. FEBS Lett 399:267–271

Seydel U, Ulmer AJ, Uhlig S, Rietschel ET (1999) Lipopolysaccharide, a membrane-forming and inflammation-inducing bacterial macromolecule. In: Zimmer G (ed) Membrane structure in disease and drug therapy. Marcel Dekker, New York, pp 217–254

Seydel U, Oikawa M, Fukase K, Kusumoto S, Brandenburg K (2000) Intrinsic conformation of lipid A is responsible for agonistic and antagonistic activity. Eur J Biochem 267:3032–3039

Snyder DS, McIntosh TJ (2000) The lipopolysaccharide barrier: correlation of antibiotic susceptibility with antibiotic permeability and fluorescent probe binding kinetics. Biochemistry 39:11777–11787

Stumpe S, Schmid R, Stephens DL, Georgiou G, Bakker EP (1998) Identification of OmpT as the protease that hydrolyses the antimicrobial peptide protamine before it enters growing cells of *Escherichia coli*. J Bacteriol 180:4002–4006

Sugimura K, Nishihara T (1988) Purification, characterization, and primary structure of *Escherichia coli* protease VII with specificity for paired basic residues: identity of protease V11 and OmpT. J Bacteriol 170:5625–5632

Urbanova M, Dukor RK, Pancoska P, Gupta VP, Keiderling TA (1991) Comparison of α-lactalbumin and lysozyme using

vibrational circular dichroism. Evidence for a difference in crystal and solution structures. Biochemistry 30:10479–10485

Vandeputte-Rutten L, Kramer RA, Kroon J, Dekker N, Egmond MR, Gros P (2001) Crystal structure of the outer membrane protease OmpT from *Escherichia coli* suggests a novel catalytic site. EMBO J 20:5033–5039

Webb RM, Lundrigan MD (1996) OmpT in *Escherichia coli* correlates with severity of disease in urinary tract infection. Med Microbiol Lett 5:8–14

Wiese A, Schröder G, Brandenburg K, Hirsch A, Welte W, Seydel U (1994) Influence of the lipid matrix on incorporation and function of LPS–free porin from *Paracoccus denitrificans*. Biochim Biophys Acta 1190:231–242

Yoshimura A, Lien E, Ingalls RR, Tuomanen E, Dziarski R, Golenbock D (1999) Cutting edge: recognition of Gram-positive bacterial cell wall components by the innate immune system occurs via Toll-like receptor 2. J Immunol 163:1–5